Aromatic−Rare Gas Complexes: The Microwave Spectrum and Structure of the Fluorobenzene−Neon Dimer

Robb J. Wilson,[†] Sean A. Peebles,[†] Sonia Antolínez,[‡] M. Eugenia Sanz,[‡] and Robert L. Kuczkowski*,[†]

Department of Chemistry, The University of Michigan, Ann Arbor, Michigan 48109-1055, and Departamento de Química Física, Facultad de Ciencias, Universidad de Valladolid, 47005 Valladolid, Spain

Received: August 27, 1998; In Final Form: October 29, 1998

The rotational spectrum of the fluorobenzene−neon complex was assigned. The structure of the complex was deduced from the rotational constants of the $C_6H_5F-{}^{20}Ne$, $C_6H_5F-{}^{22}Ne$, and $C_6D_5F-{}^{20}Ne$ species. The dimer has C_s symmetry. The neon atom sits nearly above the center of the fluorobenzene at a perpendicular distance of 3.422(1) Å. It is shifted 0.13(1) Å from the center of the ring toward the fluorinated carbon atom. The structure is compared with a number of related aromatic−rare gas complexes (rare gas = Ne or Ar). Trends are discussed in view of dispersion, polarization, and repulsive forces.

1. Introduction

Rare gas dimers with an aromatic partner have been a fertile field of investigation. A number of prototype benzene-related systems with argon have been probed both experimentally and theoretically, including benzene,[1−8] fluorinated benzenes,[9−15] and aniline.[16−18] It appears that only four experimental studies involving neon have been published (benzene,[6−8,19] aniline,[17,18] 4-fluorostyrene,[20,21] and cyclopentadienyl radical[22]). We recently began a search for the fluorobenzene−water complex in our laboratory using neon as the carrier gas. Although this species has been elusive, it was not surprising given the similarity in mass that transitions from the previously unreported fluorobenzene−neon complex were readily observed in the search regions. It seemed worthwhile to add a definitive structure for fluorobenzene−neon to the database. In the process of comparing our results with other neon and argon systems in the literature, including several related heterocyclic−rare gas dimers,[23−27] some interesting trends became apparent. These trends will be discussed later in this paper after presentation of the experimental details and analysis of the rotational spectrum of fluorobenzene−neon.

2. Experimental Details

The fluorobenzene−neon dimer was generated by supersonic expansion of a gaseous mixture of approximately 5% fluorobenzene, 1.5% water (not present for the d_5 experiments), and 93.5% carrier gas (∼90% Ne, 10% He was used for all isotopomers) at a total pressure between 1.5 and 2.8 atm. Fluorobenzene−^{20}Ne (90.9%) and fluorobenzene−^{22}Ne (8.8%) were observed in natural abundance. Fluorobenzene-d_5 (Cambridge Isotope Labs, 98% D) was used to observe the $C_6D_5F-{}^{20}Ne$ complex.

The rotational microwave spectra were recorded with a Balle−Flygare type FT microwave spectrometer operating between 4 and 18 GHz, with a modified Bosch fuel injector serving as the pulsed supersonic nozzle.[28] The gas expansion axis was perpendicular to the microwave cavity axis, providing average line widths of 30 kHz, full-width at half-maximum. Peak frequencies were reproducible to within 4−5 kHz. Stark-effect splittings were observed by applying dc voltages of up to 5.0 kV of opposite polarity to two parallel steel mesh plates (about 30 cm apart).[29] The $J = 0 \rightarrow 1$ transition of OCS was used as a calibration standard (μ(OCS) = 0.71520 D).[30]

3. Results

3.1. Spectra. The $J = 2 \rightarrow 3$ transitions around 8 GHz were first observed in a region where transitions of $C_6H_5F{\cdot}H_2O$ (nearly the same mass) were expected. When these transitions did not appear in mixtures using argon as the bath gas, they were attributed to C_6H_5F-Ne, an assignment which eventually was confirmed through the use of additional isotopes. Both *a*- and *b*-type transitions were observed. The assignments of the spectra were guided by spectral predictions based on estimated structures and by Stark effects of selected transitions. No *c*-type lines were found, although searches were made close to the predicted frequencies. Table 1 lists the observed frequencies for the normal species isotopomer ($C_6H_5F-{}^{20}Ne$). They were fit with an S-reduced Watson Hamiltonian (I^r representation). The calculated rotational constants and other spectroscopic parameters are given in Table 2.

To ascertain the structure of the dimer, the spectra of two other isotopomers were assigned. The spectra of the ^{22}Ne species (Table 3) and the fully deuterated species (Table 4) were assigned. All isotopomers had *a*- and *b*-type transitions. Quadrupole splitting was not observed in the deuterated spectrum, although line broadening was noticeable but unresolvable. This is presumably the basis for the slightly poorer fit of the transitions.

3.2. Dipole Moment. The second-order Stark effects of four *M* components of three rotational transitions of fluorobenzene−^{20}Ne were measured. The transitions were carefully selected to minimize effects from nonlinear (i.e., nonsecond-order) effects and from calibration and measurement errors at low fields. The Stark coefficients ($\Delta\nu/\epsilon^2$) were fit by a least-squares method using perturbation coefficients calculated from the spectroscopic constants to give $|\mu_A| = 1.093(13)$ D, $|\mu_B| = 1.080(10)$ D, and

* Corresponding author.
† The University of Michigan.
‡ Universidad de Valladolid.

10.1021/jp9835519 CCC: $15.00
Published on Web 12/09/1998

TABLE 1: Observed Rotational Transition Frequencies for Fluorobenzene−^{20}Ne

transition								
J'	K_a'	K_c'	−	J''	K_a''	K_c''	ν_{obs}/MHz	$\Delta\nu^a$/MHz
2	0	2	−	1	1	1	5372.688	0.000
2	1	2	−	1	1	1	5484.266	0.000
2	0	2	−	1	0	1	5653.972	−0.003
2	1	2	−	1	0	1	5765.551	−0.001
2	1	1	−	1	1	0	6214.706	−0.001
2	2	1	−	1	1	0	7058.473	0.000
2	2	0	−	1	1	1	7619.119	0.001
2	2	0	−	1	0	1	7900.405	0.000
3	0	3	−	2	1	2	8093.001	0.002
3	1	3	−	2	1	2	8123.597	−0.002
3	0	3	−	2	0	2	8204.576	0.000
3	1	3	−	2	0	2	8235.176	−0.001
3	1	2	−	2	2	1	8297.343	0.002
3	2	2	−	2	2	1	8774.196	0.001
3	1	2	−	2	1	1	9141.107	−0.001
3	2	1	−	2	2	0	9342.028	0.000
3	2	2	−	2	1	1	9617.968	0.006
4	0	4	−	3	1	3	10704.884	0.001
3	3	1	−	2	2	0	10998.680	0.000
3	3	0	−	2	2	1	11270.992	−0.001
3	2	1	−	2	1	2	11476.879	−0.001
4	2	3	−	3	1	2	12010.070	−0.003

[a] $\Delta\nu = \nu_{obs} - \nu_{calc}$, where ν_{calc} was obtained with the corresponding constants in Table 2.

$|\mu_T| = 1.536(20)$ D (Table 5). These values make sense in light of the structure discussed below. The fluorobenzene is at about a 45° angle to the *a* and *b* axes, so its dipole moment will be projected on each axis approximately equally. The magnitude of the total moment is slightly smaller than the monomer value of 1.555(3) D,[10] as one would expect if polarization effects are small and vibrational averaging effects slightly reduce the monomer value.[31]

3.3. Structure. The structure of the complex was initially assumed to be similar to that of the argon analog, a stacked structure with the neon above the ring and in the perpendicular symmetry plane of the fluorobenzene. The plane of symmetry can be established by examining the planar moments of the complex. Comparison of the out-of-plane second moment ($P_{cc} = \sum m_i c_i^2$) of the normal (87.305 amu Å^2) and the ^{22}Ne (87.267 amu Å^2) species indicates that the neon atom lies in the *ab* symmetry plane.

Figure 1 gives one representation of each of the two initial structures obtained by least-squares fitting of the six moments of inertia from the ^{20}Ne and ^{22}Ne species to two parameters. Figure 1 illustrates the relevant structural parameters that define the structure. The two most important ones are $R_\perp$ and $R_\parallel$. $R_\perp$ is the perpendicular distance of the neon from the plane of the ring. $R_\parallel$ is the distance of the neon from the center-of-mass of fluorobenzene, along its C_2 axis. The two structures differ in the direction of $R_\parallel$, either toward the fluorine or away. Alternatively, the distance of neon from the center-of-mass of fluorobenzene (called R_{cm}) and the tilt angle that R_{cm} makes with the *c* axis of the fluorobenzene monomer (called θ) can be used. Careful inspection will discern that the neon is closer to the fluorine in the top structure, while closer to the center of the aromatic ring in the bottom structure. In essence, this difference arises because only the absolute value of the neon coordinates is obtained from analyzing the two neon isotopic spectra. This structural ambiguity was resolved after assignment of the $C_6D_5F-^{20}Ne$ isotopomer. As Table 6 illustrates, the two structures predicted significantly different rotational constants for this species leading to identification of structure **II** as the correct species.

The values of the four parameters (only two are independent) obtained from least-squares fitting of the nine moments of inertia and the principal axis coordinates of all the atoms are given in Table 7. The monomer structure was assumed to be unchanged upon dimerization.[33] The fit ($\Delta I_{rms} = 1.66$ amu Å^2) is quite poor due to the large-amplitude vibrational motions that affect the moments of inertia but are neglected in the fitting procedure.

Klots et al.[23] developed a more rigorous model to account for large amplitude wagging motions specifically in aromatic−rare gas complexes. Bauder et al.[24,25] refined the model further. In simple terms, the model assumes vibrational motions α_x and α_y and assumes they are equal (which is true for a symmetrical aromatic). This motion is then expressed as a precession around the *c* axis of the monomer and averaged (see Figure 2). The monomer inertial tensor (with the inertial axis origin coincident with the monomer center-of-mass) is then recalculated based on this motion. It is then, in the second step, relocated to a parallel axis system with its origin at the complex center-of-mass. Finally, the inertial tensor is transformed, by diagonalization, to the principal axis system of the complex. The structural parameters, R_{cm}, θ, and $\langle\alpha\rangle$ are then fit to the experimental moments of inertia for the monomer and the complex.

The equations which are used to obtain R_{cm}, θ, and $\langle\alpha\rangle$ are

$$I_{xx}^C = \frac{1}{2}(\langle I_{xx}^M\rangle + \langle I_{zz}^M\rangle + \mu R^2) + \frac{1}{2}(\langle I_{xx}^M\rangle - \langle I_{zz}^M\rangle + \mu R^2 \cos 2\theta)(1 + \tan^2 2\gamma)^{1/2}$$

$$I_{yy}^C = \langle I_{yy}^M\rangle + \mu R^2$$

$$I_{zz}^C = \frac{1}{2}(\langle I_{xx}^M\rangle + \langle I_{zz}^M\rangle + \mu R^2) - \frac{1}{2}(\langle I_{xx}^M\rangle - \langle I_{zz}^M\rangle + \mu R^2 \cos 2\theta)(1 + \tan^2 2\gamma)^{1/2}$$

where

$$\tan^2 2\gamma = \frac{2I_{xz}}{(\langle I_{zz}^M\rangle - \langle I_{xx}^M\rangle - \mu R^2 \cos 2\theta)}$$

and I_{ii}^C are the experimental moments of the complex, and I_{ii}^M are the experimental moments of the monomer as a function of $\langle\alpha\rangle$. R_{cm}, θ, and μ have their usual meanings. A nonlinear equations fitting program was developed to determine R_{cm}, θ, and $\langle\alpha\rangle$ for fluorobenzene−neon. The program was later checked against a Mathematica-based program obtained from Bauder.[34] The values obtained in Table 8 for fluorobenzene−neon do not differ markedly from the values in Table 7, except for the wagging angle α; nevertheless, they are considered better approximations of the so-called r_0, or effective, parameters in the ground vibrational state.

4. Discussion

4.1. Interaction Forces. The use of the fluorobenzene-d_5 isotopic data was essential to resolving the structural ambiguity arising with the normal species data alone. This structural ambiguity has been illustrated in Figure 1. Only structure **II** is compatible with the data, indicating that the neon is nearly over the center of the fluorobenzene ring. Compared to benzene−neon, the principal effect of the fluorine has been to shift the neon about 0.13 Å from the center of the ring toward C_1, or alternatively 0.39 Å from the center-of-mass of the fluorobenzene, away from C_1.

TABLE 2: Spectroscopic Constants for Fluorobenzene−Neon Isotopomers

	fluorobenzene−^{20}Ne	fluorobenzene−^{22}Ne	fluorobenzene-d_5−^{20}Ne
A/MHz	1926.421(2)	1889.8299(4)	1742.194(2)
B/MHz	1645.236(3)	1590.8250(7)	1516.882(2)
C/MHz	1279.734(1)	1230.9208(3)	1227.862(1)
D_J/kHz	25.45(9)	23.00(3)	16.77(2)
D_{JK}/kHz	−89.8(4)	−70.9(2)	−46.89(9)
D_K/kHz	112.7(4)	88.6(2)	64.1(1)
d_1/kHz	−8.79(6)	−8.22(2)	−5.27(2)
d_2/kHz	1.28(3)	0.65(2)	0.84(1)
n^a	22	15	48
$\Delta\nu_{rms}$/kHz^b	1.8	1.1	13.3
P_{aa}/amu Å^2	219.873	230.417	227.340
P_{bb}/amu Å^2	175.036	180.153	184.253
P_{cc}/amu Å^2	87.305	87.267	105.829

[a] Number of transitions in the fit. [b] $\Delta\nu = \nu_{obs} - \nu_{calc}$.

TABLE 3: Observed Rotational Transition Frequencies for Fluorobenzene−^{22}Ne

transition								
J'	K_a'	K_c'	−	J''	K_a''	K_c''	ν_{obs}/MHz	$\Delta\nu^a$/MHz
2	2	1	−	1	1	0	6899.922	−0.001
2	2	0	−	1	1	1	7444.555	−0.001
2	2	0	−	1	0	1	7743.648	0.001
3	0	3	−	2	1	2	7791.320	0.000
3	1	3	−	2	1	2	7827.422	0.000
3	0	3	−	2	0	2	7915.818	0.001
3	1	2	−	2	2	1	7938.830	0.000
3	1	3	−	2	0	2	7951.917	−0.001
3	1	2	−	2	1	1	8836.072	0.000
4	0	4	−	3	1	3	10311.845	−0.001
4	1	4	−	3	1	3	10320.503	0.000
4	0	4	−	3	0	3	10347.948	0.000
4	1	4	−	3	0	3	10356.606	0.001
3	3	1	−	2	2	0	10769.747	0.000
3	3	0	−	2	2	1	11023.827	0.000

[a] $\Delta\nu=\nu_{obs} - \nu_{calc}$, where ν_{calc} was obtained with the corresponding constants in Table 2.

The two attractive forces that influence the location of the neon are dispersion and polarization. The polarization interaction will be maximized in regions of high electrostatic potential, while dispersion forces favor interactions with the maximum number of atoms. Ab initio calculations on fluorobenzene in our lab indicate that the regions of highest electrostatic potential and therefore greatest polarizing forces are in the plane of the ring.[35] However, dispersion is maximized at sites above the aromatic ring, where the rare gas can more closely approach several atoms. Thus, we conclude that the dispersion effect is the dominant interaction in placing the rare gas above the ring whereas the interaction of the neon-induced dipole with the fluorobenzene moments is small and fine tunes the placement. It is interesting that, at a distance of 3.0−3.5 Å above the ring, the electrostatic potential is least negative in the region between the center of the ring and C_1(F), which correlates with the location of the rare gas. This is consistent with a small contribution from polarization.

This qualitative analysis is supported by ideas in a pair of seminal papers by Kraka, Cremer, et al.[26,27] on the argon−oxazole and argon−isoxazole complexes. In these papers, the analysis of the rotational spectrum was complemented by high-level ab initio supermolecule calculations similar to other calculations on benzene−rare gas complexes,[3−7] fluorobenzene−argon,[11] and 1,4-difluorobenzene−argon.[11] However, the Kraka−Cremer papers also included a detailed charge density analysis of benzene−argon before and after complexation. From this analysis, they conclude that dispersion interactions and exchange repulsion play a major role and polarization a minor

TABLE 4: Observed Rotational Transition Frequencies for Fluorobenzene-d_5−^{20}Ne

transition								
J'	K_a'	K_c'	−	J''	K_a''	K_c''	ν_{obs}/MHz	$\Delta\nu^a$/MHz
2	1	2	−	1	1	1	5200.285	0.016
2	0	2	−	1	0	1	5335.602	0.014
2	1	2	−	1	0	1	5425.651	0.015
2	1	1	−	1	1	0	5778.002	−0.022
2	2	1	−	1	1	0	6453.981	−0.028
2	2	0	−	1	1	1	6896.379	−0.052
3	0	3	−	2	1	2	7694.803	0.008
3	1	3	−	2	1	2	7719.660	0.004
3	0	3	−	2	0	2	7784.854	0.011
3	1	3	−	2	0	2	7809.709	0.005
3	1	2	−	2	2	1	7849.518	−0.022
3	2	2	−	2	2	1	8233.488	0.007
3	1	2	−	2	1	1	8525.527	0.004
3	2	1	−	2	2	0	8681.179	−0.028
3	2	2	−	2	1	1	8909.446	−0.019
3	3	1	−	2	2	0	10007.997	0.007
4	0	4	−	3	1	3	10192.824	0.001
4	1	4	−	3	1	3	10198.496	−0.003
4	0	4	−	3	0	3	10217.682	−0.002
3	3	0	−	2	2	1	10221.477	−0.001
4	1	4	−	3	0	3	10223.359	0.000
3	2	1	−	2	1	2[b]	10377.443	0.072
4	1	3	−	3	2	2	10692.711	−0.010
4	2	3	−	3	2	2	10848.170	−0.016
4	1	3	−	3	1	2	11076.670	0.007
4	3	2	−	3	3	1	11177.942	0.004
4	2	3	−	3	1	2	11232.137	0.009
4	3	1	−	3	3	0	11453.151	0.009
4	2	2	−	3	2	1	11586.226	0.019
4	3	2	−	3	2	1	12504.729	0.007
5	0	5	−	4	1	4	12658.344	−0.001
5	1	5	−	4	1	4	12659.524	0.002
5	0	5	−	4	0	4	12664.018	−0.001
5	1	5	−	4	0	4	12665.195	−0.003
5	1	4	−	4	2	3	13338.759	0.020
5	2	4	−	4	2	3	13386.185	0.001
5	2	3	−	4	3	2	13391.600	−0.004
4	3	1	−	3	2	2	13441.110	−0.028
5	1	4	−	4	1	3	13494.205	0.001
5	2	4	−	4	1	3	13541.639	−0.010
4	4	1	−	3	3	0	13549.810	−0.007
4	4	0	−	3	3	1	13629.271	0.010
4	3	1	−	3	1	2	13825.081	0.001
5	3	3	−	4	3	2	13893.340	−0.012
5	4	2	−	4	4	1	14053.451	−0.004
5	4	1	−	4	4	0	14181.662	0.003
5	2	3	−	4	2	2	14310.110	−0.008
5	3	2	−	4	3	1	14492.908	0.005
5	3	3	−	4	2	2	14811.870	0.004

[a] $\Delta\nu = \nu_{obs} - \nu_{calc}$, where ν_{calc} was obtained with the corresponding constants in Table 2. [b] This transition was not included in the fit due to a large uncertainty in the measurement.

TABLE 5: Stark Coefficients and Dipole Moment of Fluorobenzene−^{20}Ne

transition	|M|	$(\Delta\nu/\epsilon^2)$ (obs) MHz/(kV/cm)^2	(obs − calc) MHz/(kV/cm)^2
$2_{21}-1_{10}$	0	15.06(20)	−0.002
$3_{21}-2_{12}$	0	−6.440(50)	−0.038
	1	22.10(40)	0.000
$3_{13}-2_{12}$	0	−1.955(20)	−0.050

$|\mu_a| = 1.093(13)$ D
$|\mu_b| = 1.080(10)$ D
$|\mu_T| = 1.536(20)$ D

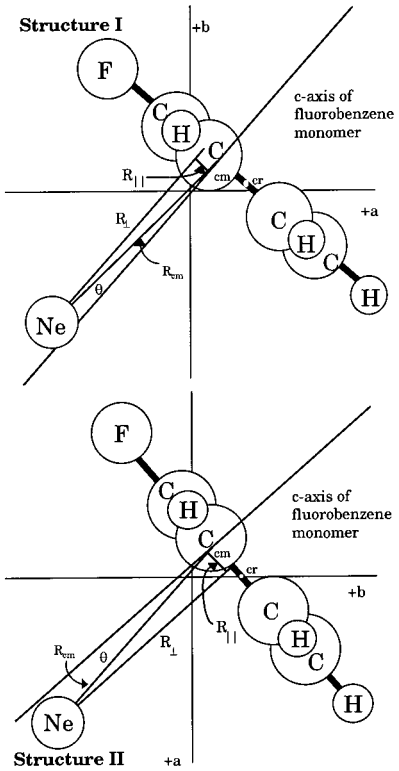

Figure 1. Two possible structures of fluorobenzene−neon, showing most of the relevant structural parameters. Only structure **II** is consistent with all of the isotopic data.

TABLE 6: Comparison of Experimental Rotational Constants of the Fluorobenzene-d_5−Neon Complex with Those Predicted for Two Possible Structures (MHz)

rotational constant	structure **I**	structure **II**	experiment
A	1760.132	1744.413	1742.194
B	1492.692	1512.365	1516.882
C	1234.123	1239.624	1227.862

role in situating the rare gas above the ring plane. Moreover, the drive to minimize exchange repulsion plays a crucial role in determining the position of argon above the ring. In benzene, attractive dispersion forces are greatest over carbon atoms while the destabilizing charge repulsion is smallest over the ring center. The observed C_{6v} symmetry of benzene−rare gas implies that the drive to minimize the exchange repulsion forces directs the rare gas to the center of the ring, where compensating dispersion and polarizing interactions are encountered with all six carbon atoms.

These ideas were carried over to the oxazole[26] and isoxazole[27] systems, which contain electronegative atoms in the ring. In oxazole, the argon adopts a position above the ring plane (3.46 Å, shorter than that in benzene−argon) and is shifted from the center of the ring toward the oxygen atom. This maximizes the

TABLE 7: Structural Parameters and Principal Axis Coordinates of Fluorobenzene−Neon[a]

parameter	value
R_{cm}/Å	3.448(7)
θ/degree	6.6(2)
Ne−ring dist/Å ($R_\perp$)	3.426(7)
$R_{||}$/Å	−0.39(1)[b]
ΔI_{rms}/amu Å^2 [c]	1.66

	coordinates in principal axis system		
	a/Å	*b*/Å	*c*/Å
F_1	−2.087	−1.079	0.000
H_2	−0.986	−0.091	−2.158
H_3	0.849	1.554	−2.151
H_4	1.778	2.387	0.000
H_5	0.849	1.554	2.151
H_6	−0.986	−0.091	2.158
C_1	−1.079	−0.175	0.000
C_2	−0.589	0.265	−1.218
C_3	0.451	1.197	−1.209
C_4	0.974	1.666	0.000
C_5	0.451	1.197	1.209
C_6	−0.589	0.265	1.218
X_{cm}[d]	−0.444	0.394	0.000
X_{cr}	−0.053	0.745	0.000
Ne	2.136	−1.893	0.000

[a] Obtained by least-squares fitting of the nine moments of inertia. For comparison, the Kraitchman single substitution coordinates[32] (absolute values, in Å) for the neon are (2.181, 1.794). The *c* coordinate is assumed to be zero. [b] (−) indicates a shift from the fluorobenzene center-of-mass toward the ring center. [c] $\Delta I = [I_{x(obs)} - I_{x(calc)}]$, where I_x is one of the observed moments of inertia. [d] X_{cm} is the center-of-mass, and X_{cr} is the center of the ring of the fluorobenzene monomer.

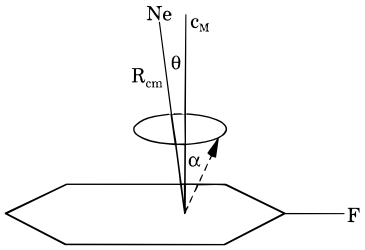

Figure 2. Definitions of structural parameters used in Table 8 (Bauder equations): R_{cm}, θ, and $\langle\alpha\rangle$. c_M represents the *c* axis of the principal coordinate system of the aromatic monomer.

dispersion interaction, while the argon moves toward the atom with the smallest volume and the smallest exchange repulsion, viz., oxygen. The Kraka−Cremer papers note that the electron density provides an excellent tool to unravel the electronic factors that determine the minimum-energy structure of a van der Waals complex.

By analogy, the extension of these ideas to the fluorobenzene−neon complex are nicely consistent with the observed structure. It is inferred that the position of the neon above the ring but shifted slightly from the ring center toward the more electron-deficient fluorinated carbon atom is a result of the lower exchange repulsion forces in this region. This is consistent with the smaller electrostatic potential in this region, mentioned above. The ab initio calculation on the fluorobenzene−argon system[11] did not explore the charge density distribution in the complex. It employed a small basis set and its main purpose was to confirm the basic results from the experimental study—viz., argon about 3.6 Å above the ring and shifted 0.33−0.43 Å from the center-of-mass of fluorobenzene. It did point out the flatness of the stabilization energy upon fluorination (i.e., the stabilization energies of the fluorobenzene and 1,4-difluo-

TABLE 8: Comparison of Structural Parameters[a] of Aromatic−RG Complexes[a]

complex	$R_\perp$	$R_\parallel$	R_{cm}	θ	$\langle\alpha\rangle$	ref
Cp−^{20}Ne	3.58	0.00	3.58	0.00	0.00	22
benzene−^{20}Ne	3.462	0.00	3.462	0.00	6.6	8
fbz−^{20}Ne	3.422	0.393	3.445	6.56	12.0	this work
fbz−^{22}Ne	3.422	0.376	3.442	6.22	12.1	this work
fbz-d_5−^{20}Ne	3.407[b]	0.368[b]	3.437[b]	6.15[b]	10.8[b]	this work
benzene−Ar	3.586	0.00	3.586	0.00	4.81	8
fbz−Ar	3.572	0.297	3.584	4.8	9.92	24
1,4-dfbz−Ar	3.550	0.00	3.550	0.00	0.00	12
1,2-dfbz−Ar	3.545	0.523[c]	3.583	8.4	7.38	24
1,2,3-tfbz−Ar	3.522	0.532	3.562	8.593	4.63	39,15

[a] R_{cm}, θ, and $\langle a\rangle$ are calculated using the equations in the text from Bauder et al.[25] except for Cp−Ne, benzene−Ne, Ar, and 1,4-dfbz−Ar. $R_\perp$ and $R_\parallel$ are calculated from R_{cm} and θ. $R_\perp$ is the perpendicular distance of the rare gas above the ring. $R_\parallel$ is the distance the rare gas is displaced parallel to the ring plane from the center-of-mass of the ring toward the ring center; see Figure 1. Uncertainties are discussed in the text. Cp = C_5H_5, fbz = fluorobenzene, dfbz = difluorobenzene, tfbz = trifluorobenzene. [b] These parameters should be identical for all three isotopomers of fluorobenzene−neon to first order. Hence, residual model errors (of about 0.01 Å) are from neglected vibrations. The parameters are corrected to the center-of-mass coordinate system of normal fluorobenzene−neon. [c] There is insufficient isotopic data to unambiguously determine the direction of $R_\parallel$.

robenzene complexes are only slightly smaller than that of benzene). Also, the intermolecular distances were very slightly affected.

It should be noted that an alternative rationale emphasizing polarization effects might also be considered. Thus, the shift of the Ne toward the fluorine end compared to benzene may be simply a consequence of the large dipole moment in fluorobenzene, which could be responsible for nudging the rare gas toward the substituted end, as well as a slightly shorter R_{cm}. Dykstra has pointed out the importance of polarization effects in rationalizing structural trends in a number of studies.[36−38] In the next section, the possibility of obtaining additional insights from a careful comparative analysis of some other rare gas−aromatic van der Waals complexes will be explored.

4.2. Comparison of Structures. This study motivated us to compare the fluorobenzene−neon structure with other related systems to discern the effect of fluorination on the interaction. To make meaningful comparisons, the structures were analyzed using a common model, viz., the Bauder model, insofar as possible. The systems that were chosen are listed in Table 8. Before discussing the comparisons, it is appropriate to explore first the methodology and assumptions used to derive structures from spectroscopic data and uncertainties that arise. The methodology often employed is to fit the ground-state (vibrationally averaged) moments of inertia to several structural parameters giving a so-called r_0 (effective) structure as carried out in Table 7. Uncertainties arise principally from three sources: (i) the experimental uncertainties arising from the frequency measurements and the Hamiltonian model employed to fit each isotopic species; (ii) statistical uncertainties from least-squares fitting the moments of several isotopic species to a rigid structural model, which are the uncertainties listed in Table 7; (iii) breakdown in underlying assumptions in the structural model that is used. The assumption that breaks down is the neglect of isotope effects on vibrational motions that subtly affect the moments of inertia and degrade the results. (Note that errors from ii and iii are not entirely separable.)

In the case of van der Waals molecules, the uncertainties from i are usually small, approximately 0.0001−0.001 Å. Because of the large-amplitude motions in these weakly bonded systems, the uncertainties from ii and iii can be sizable unless care is taken in the analysis. In the case of fluorobenzene−neon, using the Bauder model, the uncertainties from i for R_{cm}, $R_\perp$, and $R_\parallel$ for the ^{20}Ne, ^{22}Ne, and fluorobenzene-d_5−^{20}Ne isotopomers are about 0.001 Å, and these are the uncertainties listed in the Abstract. Strictly speaking, uncertainties from least-squares fitting of multiple isotopic species do not apply here, since each isotope is handled separately and three parameters are fit to the three moments of inertia. The uncertainties from iii can be gauged by comparing fluorobenzene−^{20}Ne and fluorobenzene−^{22}Ne; they range from about 0.003 Å in R_{cm} and $R_\perp$ to about 0.02 Å in $R_\parallel$, based on the differences in their values, which should be identical. The fluorobenzene-d_5−^{20}Ne values differ a little more, indicating that the vibrational correction model of Bauder begins to break down further with heavy deuteration, because other vibrational modes (especially the stretching motion between fluorobenzene and neon) have been ignored. Indeed, the smaller values for R_{cm}, θ, $R_\perp$, and $R_\parallel$ for this isotopomer are consistent with a vibrational "shrinkage effect" upon deuteration. In summary, the internal consistency among the three systems indicates that comparisons between species with presumably similar large-amplitude vibrations analyzed in the same way by these fitting equations should probably be meaningful to an uncertainty of about 0.01−0.02 Å. Apart from fluorobenzene−neon and a few other systems in Table 8, the uncertainties have not been reported in the literature. Nevertheless, it is felt from the quality of the spectroscopic data and the fits that similar uncertainties [0.001 Å from i and 0.01−0.02 Å from iii] are reasonable for these systems.

All the structures in Table 8 are vibrationally averaged structures in the ground vibrational state (so-called r_0 or "effective" values). We estimate that these values may deviate as much as 3−4% from the equilibrium values. This is an educated guess based on comparison of so-called experimental values for r_e and ab initio values for the prototype benzene−argon complex.[40] Since a true experimental value for benzene−argon has yet to be determined (all reported values depend on an assumed potential function) and uncertainties in ab initio calculations are rarely reported and difficult to infer, it is unclear how to assess the various experimental and ab initio values for r_e and compare them to r_0.

Thus, in light of this discussion and qualifying our remarks accordingly, an attempt is made here to note potentially meaningful trends within the class of aromatic−RG (RG = Ne or Ar) van der Waals dimers. Since all the data in Table 8 have been derived using the same structural model, there is good reason to presume that trends and differences, even small ones, will be reflected also in the true equilibrium values if they become available. Values for $R_\perp$ will be primarily discussed, since this more directly reflects electronic effects. It is initially noted that the argon−aromatic distances are longer than the corresponding neon−aromatic distances by about 0.12−0.15 Å, given the larger size of the argon atom. This is a typical result for argon/neon systems.

For both argon and neon, the benzene dimer shows a slightly longer $R_\perp$ than the fluorobenzene dimer with the effect more definitively established in the neon complex. This indicates that the electron-withdrawing effect of the fluorine on the ring induces a slightly closer approach between the ring and the rare gas, and in fact, additional fluorine substitution on the ring further shortens the approach in the argon series. At first glance, this appears counterintuitive to simple chemical intuition; fluorination is usually expected to reduce the polarizability of hydrocarbons and their attractive interactions with other species.

However, this pattern of closer approach with fluorination and the shift of the rare gas from the ring center toward the fluorinated carbon can be considered as consistent with Kraka and Cremer's argument about the importance of repulsion effects.[26,27] More specifically, a simple interpretation of this might argue that the electron-withdrawing effect of the fluorines reduces the electron−electron repulsion between the ring and the rare gas, allowing the rare gas to approach more closely and shift toward the fluorinated carbon sites.

As noted above, one should consider whether these trends might also arise from the dipolar (and higher order) fields in the polar fluorobenzenes interacting with the rare gas and shifting it in the observed directions. This seems less attractive as the major mechanism. As pointed out earlier, ab initio calculations in our lab indicate a comparatively small electrostatic potential in fluorobenzene in the region above the ring between C_1(F) and the ring center. Nevertheless, it is difficult to separate the relative importance of the repulsion versus polarization effects with the data available. This will likely be best resolved by careful analysis of ab initio calculations on these systems.

In conclusion, the fluorobenzene−neon system exhibits a structure consistent with one intuitively based on maximizing the dispersion interaction and minimizing repulsive interactions. Related aromatic−rare gas complexes also manifest trends consistent with this description and lend substance to the hypothesis of the critical importance of repulsive interactions as an organizing principle in understanding structural trends. It would be interesting to explore a few other complexes to further test these ideas, including chlorobenzene−RG, to evaluate the effect of a larger, more polarizable but less electronegative substituent, and toluene−RG, where the substituent is an electron donor. The limiting shrinkage effect in perfluorobenzene−argon/neon would also be an interesting quantity, although this system may have to be observed by a technique other than microwave spectroscopy. Of course, the observed trends might be rationalized by any model that invokes a larger attractive force on the rare gas as electronegative or electron-rich moieties are introduced. Hence, any additional experimental or theoretical test that might help distinguish between alternative hypotheses would be welcome.

Acknowledgment. The authors gratefully acknowledge the support of the National Science Foundation (R.J.W., S.A.P., R.L.K.), Washington, DC, and FPI grants from the Ministerio de Educatíon y Cultura (S.A. and M.E.S.), Madrid, Spain. Additionally, we thank Professor A. Bauder for generously providing us with data and a copy of his program and Professor D. Cremer and Professor C. Dykstra for interesting discussions on aromatic−rare gas complexes.

References and Notes

(1) Brupbacher, Th.; Makarewicz, J.; Bauder, A. *J. Chem. Phys.* **1994**, *101*, 9736.
(2) Weber, Th.; von Bargen, A.; Riedle, E.; Neusser, H. *J. Chem. Phys.* **1990**, *92*, 90.
(3) Koch, H.; Fernandez, B.; Christiansen, O. *J. Chem. Phys.* **1998**, *108*, 2784.
(4) Hobza, P.; Bludský, O.; Selzle, H.; Schlag, E. *Chem. Phys. Lett.* **1996**, *250*, 402.
(5) Hobza, P.; Selzle, H.; Schlag, E. *J. Chem. Phys.* **1991**, *95*, 391.
(6) Hobza, P.; Bludský, O.; Selzle, H.; Schlag, E. *J. Chem. Phys.* **1992**, *97*, 335.
(7) Klopper, W.; Lüthi, H.; Brupbacher, Th.; Bauder, A. *J. Chem. Phys.* **1994**, *101*, 9747.
(8) Brupbacher, Th.; Makarewicz, J.; Bauder, A. *J. Chem. Phys.* **1994**, *101*, 9736.
(9) Stahl, W.; Grabow, J.-U. *Z. Naturforsch.* **1992**, *47a*, 681.
(10) Appleman, R.; Peebles, S.; Kuczkowski, R. *J. Mol. Struct.* **1998**, *446*, 55.
(11) Hobza, P.; Selzle, H.; Schlag, E. *J. Chem. Phys.* **1993**, *99*, 2809.
(12) Sussman, R.; Neuhauser, R.; Neusser, H. *Can. J. Phys.* **1994**, *72*, 1179.
(13) Sussmann, R.; Neusser, H. *J. Chem. Phys.* **1995**, *102*, 3055.
(14) Jochims, E.; Grabow, J.-U.; Stahl, W. *J. Mol. Struct.* **1992**, *158*, 278.
(15) Onda, M.; Bitoh, Y.; Hight-Walker, A. *J. Mol. Struct.* **1997**, *410*, 51.
(16) Sinclair, W.; Pratt, D. *J. Chem. Phys.* **1996**, *105*, 7942.
(17) Becucci, M.; Pietraperzia, G.; Lakin, N.; Castellucci, E.; Bréchignac, Ph. *Chem. Phys. Lett.* **1996**, *260*, 87.
(18) Consalvo, D.; Storm, V.; Dreizler, H. *Chem. Phys.* **1997**, *228*, 301.
(19) Arunan, E.; Emilsson, T.; Gutowsky, H. *J. Chem. Phys.* **1994**, *101*, 861.
(20) Lakin, N.; Pietraperzia, G.; Becucci, M.; Castellucci, E.; Coreno, M.; Giardini-Guidoni, A.; van der Avoird, A. *J. Chem. Phys.* **1998**, *108*, 1836.
(21) Coreno, M.; Piccirillo, S.; Giardini-Guidoni, A.; Mele, A.; Palleschi, A.; Bréchignac, Ph.; Parneix, P. *Chem. Phys. Lett.* **1995**, *236*, 580.
(22) Yu, L.; Williamson, J.; Foster, S.; Miller, T. *J. Chem. Phys.* **1992**, *97*, 5273.
(23) Klots, T.; Emilsson, T.; Ruoff, R.; Gutowsky, H. *J. Phys. Chem.* **1989**, *93*, 1255.
(24) Spycher, R.; Hausherr-Primo, L.; Grassi, G.; Bauder, A. *J. Mol. Struct.* **1995**, *351*, 7.
(25) Spycher, R.; Petitprez, D.; Bettens, F.; Bauder, A. *J. Phys. Chem.* **1994**, *98*, 11863.
(26) Kraka, E.; Cremer, D.; Spoerel, U.; Merke, I.; Stahl, W.; Dreizler, H. *J. Phys. Chem.* **1995**, *99*, 12466.
(27) Spoerel, U.; Dreizler, H.; Stahl, W.; Kraka, E.; Cremer, D. *J. Phys. Chem.* **1996**, *100*, 14298.
(28) Hillig, K., II; Matos, J.; Scioly, A.; Kuczkowski, R. *Chem. Phys. Lett.* **1987**, *133*, 359.
(29) Bohn, R.; Hillig, K., II; Kuczkowski, R. *J. Phys. Chem.* **1989**, *93*, 3456.
(30) Tanaka, K.; Ito, H.; Harada, K.; Tanaka, T. *J. Chem. Phys.* **1984**, *80*, 5893.
(31) Andrews, A.; Nemes, L.; Maruca, S.; Hillig, K., II; Kuczkowski, R.; Muenter, J. *J. Mol. Spectrosc.* **1993**, *422*, 160.
(32) Kraitchman, J. *Am. J. Phys.* **1953**, *21*, 17.
(33) Doraiswamy, S.; Sharma, S. *J. Mol. Struct.* **1983**, *102*, 81.
(34) Bauder, A. Private communication.
(35) Unpublished results, Kuczkowski lab.
(36) Dykstra, C. E. *Acc. Chem Res.* **1988**, *21*, 355.
(37) Dykstra, C. E. *J. Am. Chem. Soc.* **1989**, *111*, 6168.
(38) Dykstra, C. E. *J. Phys. Chem.* **1990**, *94*, 6498.
(39) Onda, M.; Mukaida, H.; Akiba, H.; Mori, M.; Miyazaki, H.; Yamaguchi, I. *J. Mol. Spectrosc.* **1995**, *169*, 480.

(40) Klopper et al.[7] performed an MP2-R12 calculation with counterpoise corrections for benzene−argon and obtained an equilibrium ring-gas distance (R_e) of 3.41 Å, compared with their experimental value of 3.50 Å. Note that this is different than their distance R_0 of 3.586 Å,[8] which is the ground-state vibrationally averaged value listed in Table 8. However, Weber et al.[2] estimated an experimental R_e of 3.582 Å. Brupbacher et al.[8] notes that an R_e value is highly dependent on the potential energy surface used and therefore can vary widely. Other ab initio values are 3.526 (MP2, 6-31+G*)[5,6] and 3.40 Å (CASSCF, 6-31+G*/7s4p2d1f).[6] Koch et al.[3] performed a variety of coupled cluster (CC) calculations in order to obtain accurate binding energies but did not report predicted structural data.